Acta Pharmaceutica Sinica B 2020;10(8):1397−1413

Chinese Pharmaceutical Association
Institute of Materia Medica, Chinese Academy of Medical Sciences

Acta Pharmaceutica Sinica B

www.elsevier.com/locate/apsb
www.sciencedirect.com

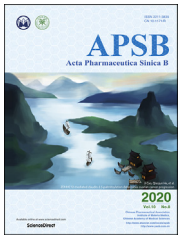

ORIGINAL ARTICLE

Miltirone induces cell death in hepatocellular carcinoma cell through GSDME-dependent pyroptosis

Xiaowei Zhang[a,b], Ping Zhang[a,b], Lin An[a,b], Ningyuan Sun[a,b], Liying Peng[a,b], Weiwei Tang[a,b], Dingyuan Ma[c,*], Jun Chen[a,b,*]

[a]*State Key Laboratory of Natural Medicines, China Pharmaceutical University, Nanjing 210009, China*
[b]*Department of Pharmacognosy, School of Traditional Chinese Pharmacy, China Pharmaceutical University, Nanjing 210009, China*
[c]*Department of Prenatal Diagnosis, Nanjing Maternity and Child Health Care Hospital, Women's Hospital of Nanjing Medical University, Nanjing 210004, China*

Received 13 April 2020; received in revised form 6 June 2020; accepted 8 June 2020

KEY WORDS

Miltirone;
Hepatocellular carcinoma;
Pyroptosis;
GSDME;

Abstract Pyroptosis is a form of programmed cell death, and recently described as a new molecular mechanism of chemotherapy drugs in the treatment of tumors. Miltirone, a derivative of phenanthrene-quinone isolated from the root of *Salvia miltiorrhiza* Bunge, has been shown to possess anti-cancer activities. Here, we found that miltirone inhibited the cell viability of either HepG2 or Hepa1-6 cells, and induced the proteolytic cleavage of gasdermin E (GSDME) in each hepatocellular carcinoma (HCC) cell

Abbreviations: 7-AAD, 7-aminoactinomycin D; ANOVA, analysis of variance; AKT, AKT serine/threonine kinase, also known as protein kinase B; BAX, BCL2-associated X; Cas9, caspase 9; CCK-8, cell counting kit-8; CRISPR, clustered regularly interspaced short palindromic repeats; DCFH-DA, dye 2,7-dichlorofluoresce diacetate; DMEM, Dulbecco's modified Eagle's medium; DMSO, dimethyl sulfoxide; ECL, enhanced chemiluminescence; ERK1/2, extracellular regulated protein kinases 1/2; FBS, fetal bovine serum; FITC, fluorescein isothiocyanate; GAPDH, glyceraldehyde-3-phosphate dehydrogenase; gRNA, guide RNA; GSDMD, gasdermin D; GSDME, gasdermin E; HCC, hepatocellular carcinoma; H&E, hematoxylin and eosin; HRP, horseradish peroxidase; IC_{50}, the half maximal inhibitory concentration; IgG (H + L), immunoglobulin G (heavy chain + light chain); i.p., intraperitoneal; i.v., intravenous; KO, knockout; LDH, lactic dehydrogenase; MEK, mitogen-activated and extracellular signal-regulated kinase; MEM, minimum essential medium; MMP, mitochondrial membrane potential; MS, mass spectrum; mTOR, mammalian target of rapamycin; NAC, *N*-acetyl cysteine; NC, negative control; N-GSDME, N-terminal GSDME; NMR, nuclear magnetic resonance; NS, no significance; p-AKT, phosphorylated-AKT; p-MEK, phosphorylated-MEK; p-ERK1/2, phosphorylated-ERK1/2; PARP, poly ADP-ribose polymerase; PBS, phosphate-based buffer; PI, propidium iodide; PI3K, phosphatidylinositol 3-kinase; RIPA, radioimmunoprecipitation assay; ROS, reactive oxygen species; SD, standard deviation; SDS-PAGE, sodium dodecyl sulphate-polyacrylamide gel electrophoresis; TBST, Tris-buffered saline with Tween solution; TCGA, the Cancer Genome Atlas; VEGF, vascular endothelial growth factor.

*Corresponding authors. Tel.: +86 25 52226309 (Dingyuan Ma); Tel.: +86 25 83271382; fax: +86 25 83271379 (Jun Chen).
E-mail addresses: dingyuanma2002@163.com (Dingyuan Ma), chenj2002cpu@126.com (Jun Chen).

Peer review under responsibility of Institute of Materia Medica, Chinese Academy of Medical Sciences and Chinese Pharmaceutical Association.

https://doi.org/10.1016/j.apsb.2020.06.015

Cell death;
HepG2;
Hepa1-6

line, with concomitant cleavage of caspase 3. Knocking out *GSDME* switched miltirone-induced cell death from pyroptosis to apoptosis. Additionally, the induction effects of miltirone on GSDME-dependent pyroptosis were attenuated by siRNA-mediated caspase three silencing and the specific caspase three inhibitor Z-DEVD-FMK, respectively. Miltirone effectively elicited intracellular accumulation of reactive oxygen species (ROS), and suppressed phosphorylation of mitogen-activated and extracellular signal-regulated kinase (MEK) and extracellular regulated protein kinases 1/2 (ERK1/2) for pyroptosis induction. Moreover, miltirone significantly inhibited tumor growth and induced pyroptosis in the Hepa1-6 mouse HCC syngeneic model. These results provide a new insight that miltirone is a potential therapeutic agent for the treatment of HCC *via* GSDME-dependent pyroptosis.

1. Introduction

Hepatocellular carcinoma (HCC), accounting for about 85%−90% of all primary liver cancers, is one of the most prevalent and lethal human malignancies worldwide, with about 841,000 new cases and 782,000 deaths annually[1,2]. Most patients with HCC are asymptomatic until the disease develops to an advanced stage, when they are ineligible for curative therapies such as liver resection or liver transplantation[3]. Systemic treatments are the important option for these HCC patients. Sorafenib, the first molecular targeted agent of HCC, has been shown to improve the survival of patients with advanced HCC[4,5]. Sorafenib is an oral multi-kinase inhibitor, and mainly targets RAF kinases and vascular endothelial growth factor (VEGF)[6,7]. Although sorafenib is the only standard clinical treatment against advanced HCC, some patients are intolerant of sorafenib, and the median survival rate is still less than one year[8]. Until now, no other agents have shown promise as the first- and second-line treatments for expanding the benefits of sorafenib therapy[9−11]. Therefore, there is an urgent need to develop new and more specific therapeutic approaches for HCC therapy.

Pyroptosis is a new form of programmed cell death characterized by cell swelling with large bubbles blowing from the plasma membrane[12,13]. Pyroptosis is initially ascribed to the proteolytic fragmentation of gasdermin D (GSDMD) by caspase 1/4/5/11[14]. Some recent study demonstrates a completely new concept that another member of gasdermin family, gasdermin E (GSDME), can switch caspase 3-mediated apoptosis induced by chemotherapy agents to pyroptosis[15]. Similar to GSDMD, GSDME contains the N- and C-terminal domains, and the N-terminal monomers oligomerize to form pores in the plasma membrane. Activated caspase three cleaves GSDME in the interdomain linker to release the N-terminal domain and form membrane pores to cause pyroptosis, as evidenced by the cell membrane ballooning, the lactic dehydrogenase (LDH) activity elevation, and the increase of propidium iodide (PI) uptake[13]. This new GSDME-dependent pyroptosis is the downstream of the activated mitochondrial-mediated caspase pathway[16] and has been proposed as a nonapoptotic mechanism to eliminate cancer cells[15].

Miltirone, an active constituent of a traditional Chinese herbal medicine *Salvia miltiorrhiza* Bunge[17], has been reported to suppress many types of tumors[18]. Miltirone was highly effective against colon cancer cells *via* inducing mitochondrial damage and the accumulation of intracellular calcium[19]. Miltirone triggered acute lymphoblastic leukemia cells apoptosis through reactive oxygen species (ROS)-generated breakdown of mitochondrial membrane potential (MMP) and DNA damage[20]. Moreover, it was reported that miltirone inhibited the growth of HCC cells and induced apoptosis in HepG2 cells[21,22]. These studies suggested that miltirone could be a potential agent for the treatment of cancer. However, the effects of miltirone on the tumor growth of HCC *in vivo* and the molecular mechanism of its anti-carcinogenesis remain to be elucidated.

In this study, we aimed to investigate the effects of miltirone on HCC *in vitro* and *in vivo*. Then, we elucidated the possible molecular mechanisms with a special focus on the ability of miltirone to induce pyroptosis against HCC. Our findings demonstrated that miltirone inhibited HCC cells growth through BCL2-associated X (BAX)−caspase−GSDME-dependent pyroptotic by regulating ROS/mitogen-activated and extracellular signal-regulated kinase (MEK)/extracellular regulated protein kinases 1/2 (ERK1/2) pathway.

2. Materials and methods

2.1. Chemicals and materials

Miltirone (Fig. 1A) was isolated from the root of *S. miltiorrhiza* Bunge (*S. miltiorrhiza*) in our laboratory. The structure was characterized by mass spectrum (MS), ^{1}H nuclear magnetic resonance (NMR), and ^{13}C NMR spectroscopic methods, and the purity of the compound was greater than 98% and re-suspended in dimethyl sulfoxide (DMSO; Sigma−Aldrich, St. Louis, MO, USA). Sorafenib was purchased from Bayer (Leverkusen, Germany). *N*-Acetyl cysteine (NAC) was from Beyotime Institute of Biotechnology (Nanjing, China). Necrostatin-1 was purchased from Sigma−Aldrich. Ceramide C6 was obtained from Santa Cruz Biotechnology (Santa Cruz, CA, USA).

2.2. Cell lines and cell culture

HepG2 cells (human HCC cells line) and Hepa1-6 cells (mouse HCC cells line) were purchased from Cell Bank of the Chinese Academy of Sciences (Shanghai, China). HepG2 and Hepa1-6 cells were cultured in minimum essential medium (MEM) and Dulbecco's modified Eagle medium (DMEM; Keygen Biotech, Nanjing, China), respectively. All the culture media were supplemented with 10% fetal bovine serum (FBS; Thermo Fisher Scientific, Waltham, MA, USA), penicillin (100 U/mL) and streptomycin (100 μg/mL; Hyclone, Logan, UT, USA). The cells were incubated at 37 °C with 5% CO_2.

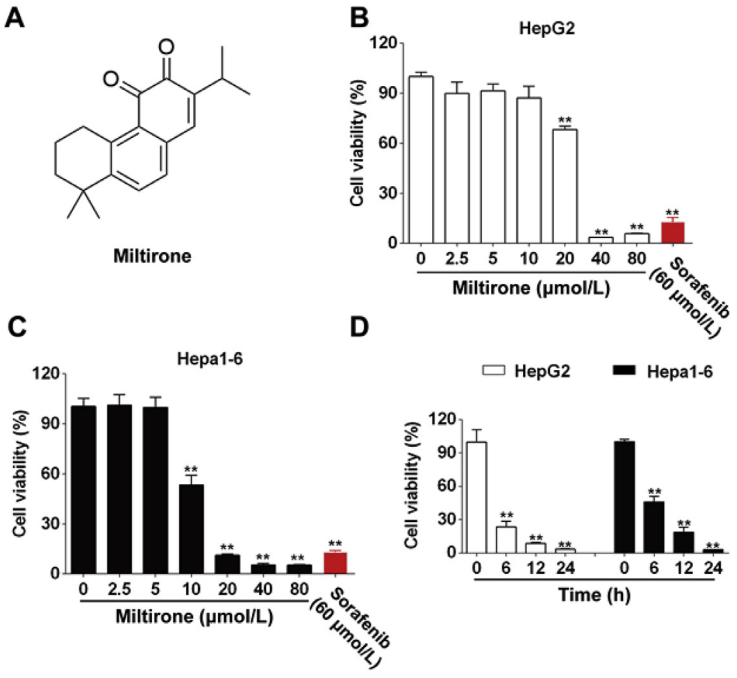

Figure 1 Miltirone inhibited the viability of HepG2 and Hepa1-6 cells in dose- and time-dependent manners. (A) Chemical structure of miltirone. (B) and (C) HepG2 and Hepa1-6 cells were treated with miltirone (0−80 μmol/L) or sorafenib (60 μmol/L) for 24 h, cell viability was analyzed by CCK-8 assay and expressed as mean ± SD ($n = 3$). (D) HepG2 and Hepa1-6 cells were treated with 40 μmol/L miltirone at indicated time, cell viability was analyzed by CCK-8 assay and expressed as mean ± SD ($n = 3$). $^{**}P < 0.01$ *vs.* control.

2.3. Clustered regularly interspaced short palindromic repeats (CRISPR)−caspase 9 (Cas9) knockout (KO) cells and siRNA knockdown

The KO cell line was generated by the CRISPR−Cas9 technology. In brief, guide RNA (gRNA) 5′-CAAGCTGCAACTTCTAAGTCT-3′ to target *Gsdme* was cloned into the pU6gRNACas9puro (pGE-2, GenePharma, Shanghai, China) to construct the pGE-2-*Gsdme*-KO plasmid. For *Gsdme* KO in Hepa1-6 cells, 2 μg pGE-2-*Gsdme*-KO plasmid was transfected into 2×10^6 Hepa1-6 cells using Lipofectamine® 2000 transfection reagent (Thermo Fisher Scientific). Forty-eight hours after the transfection, cells were selected with 1 μg/mL puromycin and the single clones were cultured in 96-well plates for another 15 days. Anti-GSDME immunoblotting was used to verify *Gsdme* KO Hepa1-6 cells.

For siRNA knockdown, Hepa1-6 cells were plated in 96- or 6-well plates. After 24 h, cells were transfected under identical conditions with caspase 3-specific siRNA duplexes (siRNA-casp3-1, siRNA-casp3-2, and siRNA-casp3-3), *Gsdmd*-specific siRNA duplexes (siRNA-GSDMD-1, siRNA-GSDMD-2, and siRNA-GSDMD-3) or control siRNA duplexes. All siRNA duplexes were purchased from Genepharma. SiRNA transfections were performed using Lipofectamine® 2000 transfection reagent according to the manufacturer's instructions. Twenty-four hours later, transfected Hepa1-6 cells were treated with miltirone (40 μmol/L) for subsequent analyses.

2.4. Cell viability assay and LDH release assay

Exponentially growing HepG2 cells or Hepa1-6 cells were seeded into 96-well plates (7×10^3 cells/well) for 24 h before stimulation. Miltirone and sorafenib were dissolved in DMSO and diluted with culture medium to various concentrations. The final concentration of DMSO was less than 0.1%, and 0.1% DMSO served as vehicle control. Cells were treated with miltirone, NAC, or sorafenib for the indicated times and concentrations. *Gsdme* KO Hepa1-6 cells were stimulated with miltirone (40 μmol/L) for 24 h. Cell viability was determined by cell counting kit-8 (CCK-8) assay (Dojindo Laboratories, Kyushu Island, Japan) as we previously reported[23]. The half maximal inhibitory concentration (IC_{50}) was calculated according to the cell viability values with Prism six software (GraphPad, San Diego, CA, USA). In other experiments, Hepa1-6 cells were pre-treated with the caspase three inhibitor (peptide Z-DEVD-FMK, MedChemExpress, Monmouth Junction, NJ, USA) for 3 h and further incubated with miltirone or vehicle control (0.2% DMSO) for 24 h and CCK-8 assay was performed. For LDH release, cell culture supernatants were collected after various treatments and the LDH activity was detected using the LDH assay kit (Beyotime Institute of Biotechnology). Briefly, the supernatants (120 μL/well) were transferred into a blank 96-well plate, and 60 μL of LDH detection reagents were added to each well. The plates were then incubated for 30 min at room temperature in the dark. The absorbance was measured at 450 nm on a spectrophotometric microplate reader (Thermo Scientific Varioskan LUX, Waltham, MA, USA).

2.5. Microscopy imaging

To examine the morphology of pyroptotic cells, Hepa1-6, *Gsdme* KO Hepa1-6 or HepG2 cells were seeded in the 6-well plate at about 60% confluency. After treated with miltirone or sorafenib, the bright-field cell images were captured using an Olympus IX53 microscope (Olympus Co., Tokyo, Japan). DMSO (0.1%) served as vehicle control.

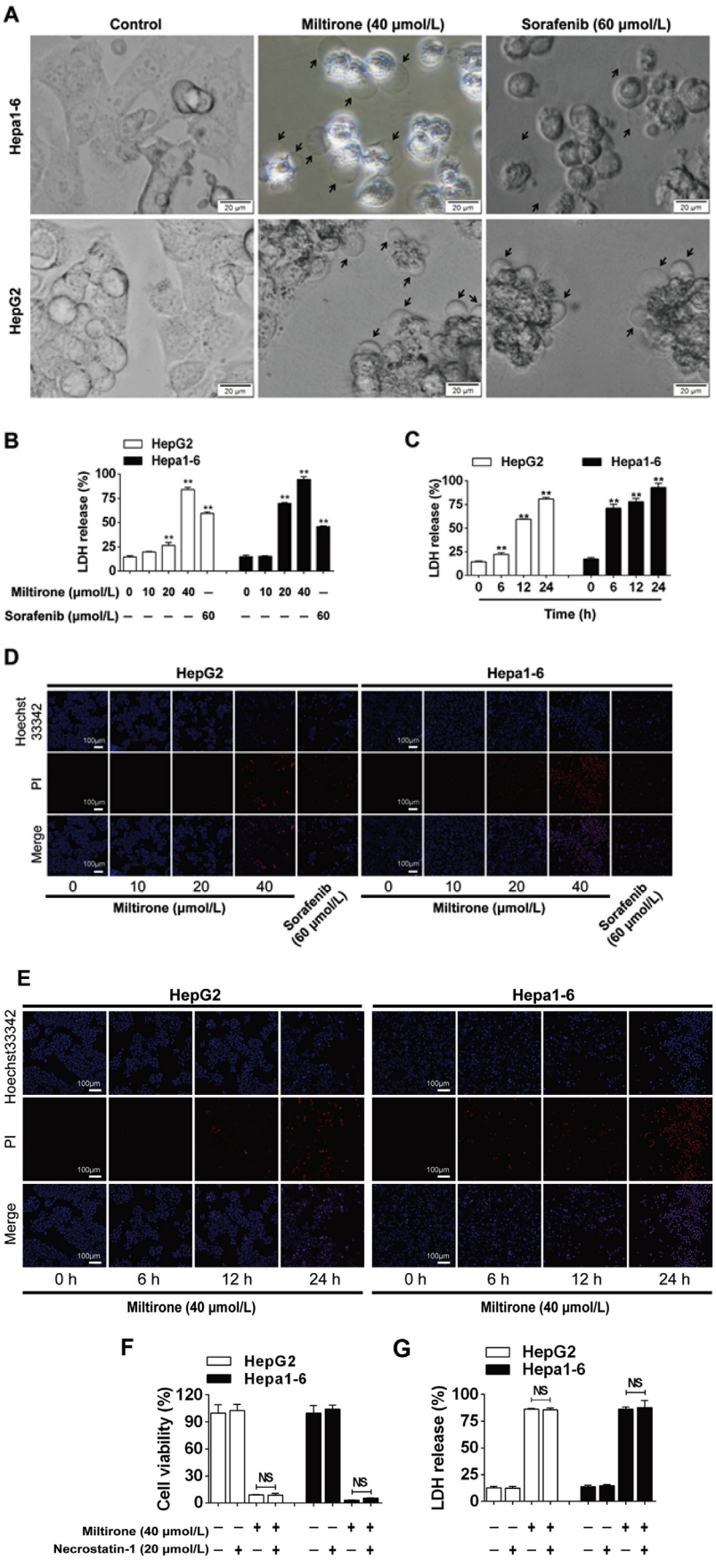
A
Control
Miltirone (40 μmol/L)
Sorafenib (60 μmol/L)
Hepa1-6
HepG2
B
HepG2
Hepa1-6
LDH release (%)
Miltirone (μmol/L) 0 10 20 40 — 0 10 20 40 —
Sorafenib (μmol/L) — — — — 60 — — — — 60
C
HepG2
Hepa1-6
LDH release (%)
0 6 12 24 0 6 12 24
Time (h)
D
HepG2
Hepa1-6
Hoechst 33342
PI
Merge
0 10 20 40
Miltirone (μmol/L)
Sorafenib (60 μmol/L)
E
HepG2
Hepa1-6
Hoechst33342
PI
Merge
0 h 6 h 12 h 24 h
Miltirone (40 μmol/L)
F
HepG2
Hepa1-6
Cell viability (%)
NS
Miltirone (40 μmol/L)
Necrostatin-1 (20 μmol/L)
G
HepG2
Hepa1-6
LDH release (%)
NS

2.6. Hoechst 33342/PI staining

Hoechst 33342/PI staining assay was performed according to the manufacturer's instructions (Apoptosis and Necrosis Assay Kit, Beyotime Institute of Biotechnology). Briefly, HepG2 and Hepa1-6 cells were cultured in 35 mm cover glass-bottom culture dishes (Corning Incorporated, Corning, NY, USA) and subjected to the indicated treatments. The final concentration of DMSO was less than 0.1%, and DMSO (0.1%) served as vehicle control. Then, Hoechst 33342 (5 μL) and PI dye (5 μL) were added and then incubated for 20 min at 4 °C in the dark and visualized under a confocal scanning microscope (Zeiss LSM 700, Jena, Germany).

2.7. Measurement of mitochondrial membrane potential ($\delta\psi_m$)

The fluorochrome dye JC-1 (Beyotime Institute of Biotechnology) was employed to measure MMP in Hepa1-6 cells. After cultured in 6-well plates, Hepa1-6 cells were treated with the indicated concentrations of miltirone (0−40 μmol/L) or sorafenib (60 μmol/L) for 24 h, and then incubated with an equal volume of JC-1 staining solution at 37 °C for 20 min. The final concentration of DMSO was less than 0.1%, and DMSO (0.1%) served as vehicle control. MMP was monitored using an Olympus IX53 microscope.

2.8. Determination of ROS production

The production of intracellular ROS was detected using fluorescent dye 2,7-dichlorofluoresce diacetate (DCFH-DA; Beyotime Institute of Biotechnology) by confocal microscopy or flow cytometer. For confocal microscopy study, Hepa1-6 cells were seeded on 35 mm cover glass-bottom culture dishes and allowed to attach for 24 h. Cells were treated with miltirone or NAC for indicated time and then loaded with DCFH-DA (10 μmol/L) in dark at 37 °C for 30 min. Fluorescent images were observed with confocal laser scanning microscope and processed using the ZEN imaging software (Zeiss, Weimar, Germany). For flow cytometry, Hepa1-6 cells were seeded in 6-well plates and treated with miltirone or NAC for indicated time. DMSO (0.1%) served as vehicle control. Then treated-cells were collected, washed with phosphate-based buffer (PBS; Hyclone) twice and stained with DCFH-DA (10 μmol/L) according to the manufacturer's instructions. Subsequently, stained cells were analyzed with flow cytometer (MACSQuant Analyzer, Miltenyi Biotec, Bergisch Gladbach, Germany) and data analyses were processed using FlowJo software.

2.9. Apoptosis evaluation by flow cytometry

Hepa1-6 and GSDME KO Hepa1-6 cells were treated with miltirone according to the indicated treatments. The final concentration of DMSO was less than 0.1%, and DMSO (0.1%) served as vehicle control. For flow cytometry detection, cells were collected, washed with PBS twice and stained using the annexin V-fluorescein isothiocyanate (FITC) and PI according to the manufacturer's instructions (Yisheng, Shanghai, China). Stained cells were analyzed with a flow cytometer (Miltenyi Biotec) and data analyses were processed using FlowJo software.

2.10. Western blotting

Cells or tumor tissues were washed with cold PBS twice and prepared in radioimmunoprecipitation assay (RIPA) lysis buffer (Beyotime Institute of Biotechnology), and Western blotting analyses were performed as following steps. Equal amount of cell or tumor tissue lysates were separated by 10% or 12% sodium dodecyl sulphate-polyacrylamide gel electrophoresis (SDS-PAGE) and transferred to nitrocellulose membranes. The membranes were then blocked with 5% skim milk in Tris-buffered saline with Tween solution (TBST, 50 mmol/L Tris-HCl, pH 8.0, 150 mmol/L NaCl, and 0.1% Tween-20) for 2 h, and then immunoblotted overnight at 4 °C with specific primary antibodies including anti-caspase 3 (1:1000, Cell Signaling Technology, Beverly, CA, USA), anti-caspase 9 (1:1000, Proteintech, Wuhan, China), anti-BAX (1:1000, Proteintech), anti-poly ADP-ribose polymerase (PARP, 1:1000, Cell Signaling Technology), anti-phosphorylated-MEK (p-MEK, 1:1000, Cell Signaling Technology), anti-phosphorylated-ERK1/2 (p-ERK1/2, 1:1000, Cell Signaling Technology), anti-MEK (1:1000, Cell Signaling Technology), anti-ERK1/2 (1:1000, Cell Signaling Technology), anti-mouse GSDMD (1:1000, Abcam, Cambridge, MA, USA), anti-human GSDMD (1:1000, Proteintech), anti-GSDME (1:1000, Abcam) and anti-glyceraldehyde-3-phosphate dehydrogenase (GAPDH, 1:5000, Abways Technology, Shanghai, China). After washing with TBST three times, membranes were incubated with the secondary antibodies of goat anti-rabbit immunoglobulin G (heavy chain + light chain)-horseradish peroxidase [IgG (H + L)-HRP, 1:10,000, Abways Technology] or goat anti-mouse IgG (H + L)-HRP (1:10,000, Abways Technology) for 2 h. Immunoreactive bands were identified using an enhanced chemiluminescence (ECL) kit (Yisheng) and visualized with the ChemiDoc XRS system (Bio-Rad, Hercules, CA, USA). Densitometry analysis for Western blotting was performed using Gelpro32 imaging software. Expression levels of proteins were normalized to total GAPDH.

2.11. Animal study

Four-to-five-week-old C57BL/6 male mice were purchased from comparative medicine center of Yangzhou University (Yangzhou, China) and maintained in the Animal Experimental Center of China Pharmaceutical University. Hepa1-6 cells (approximately 3×10^6) were injected subcutaneously into the right flank of C57BL/6 mice. Considering that miltirone is poorly absorbed with

Figure 2 Miltirone triggered pyroptosis in HCC cells (HepG2 and Hepa1-6). (A) HepG2 and Hepa1-6 cells were treated with miltirone (12 h) or sorafenib (24 h), and microscopic imaging was performed. Arrowheads indicate ballooned cell membrane characteristic of pyroptotic cells, scale bar = 20 μm. (B) HepG2 and Hepa1-6 cells were treated with miltirone or sorafenib at indicated concentrations for 24 h, LDH-release was analyzed using LDH assay kit and expressed as mean ± SD (n = 3). (C) HepG2 and Hepa1-6 cells were treated with miltirone (40 μmol/L) for 6, 12, and 24 h. LDH-release was analyzed using LDH assay kit and expressed as mean ± SD (n = 3). (D) The percentage of PI (red) positive cells were increased in HepG2 and Hepa1-6 cells after the treatment with miltirone for 24 h. Scale bar = 100 μm. (E) The percentage of PI (red) positive cells were increased in HepG2 and Hepa1-6 cells after treatment with miltirone (40 μmol/L) for 6, 12, and 24 h. Scale bar = 100 μm. (F) and (G) HepG2 and Hepa1-6 cells were treated with miltirone or necrostatin-1 for 24 h, cell viability was analyzed by CCK-8 assay, and LDH-release was analyzed using LDH assay kit and expressed as mean ± SD (n = 3). NS, no significance, $P < 0.01$ *vs.* miltirone alone.

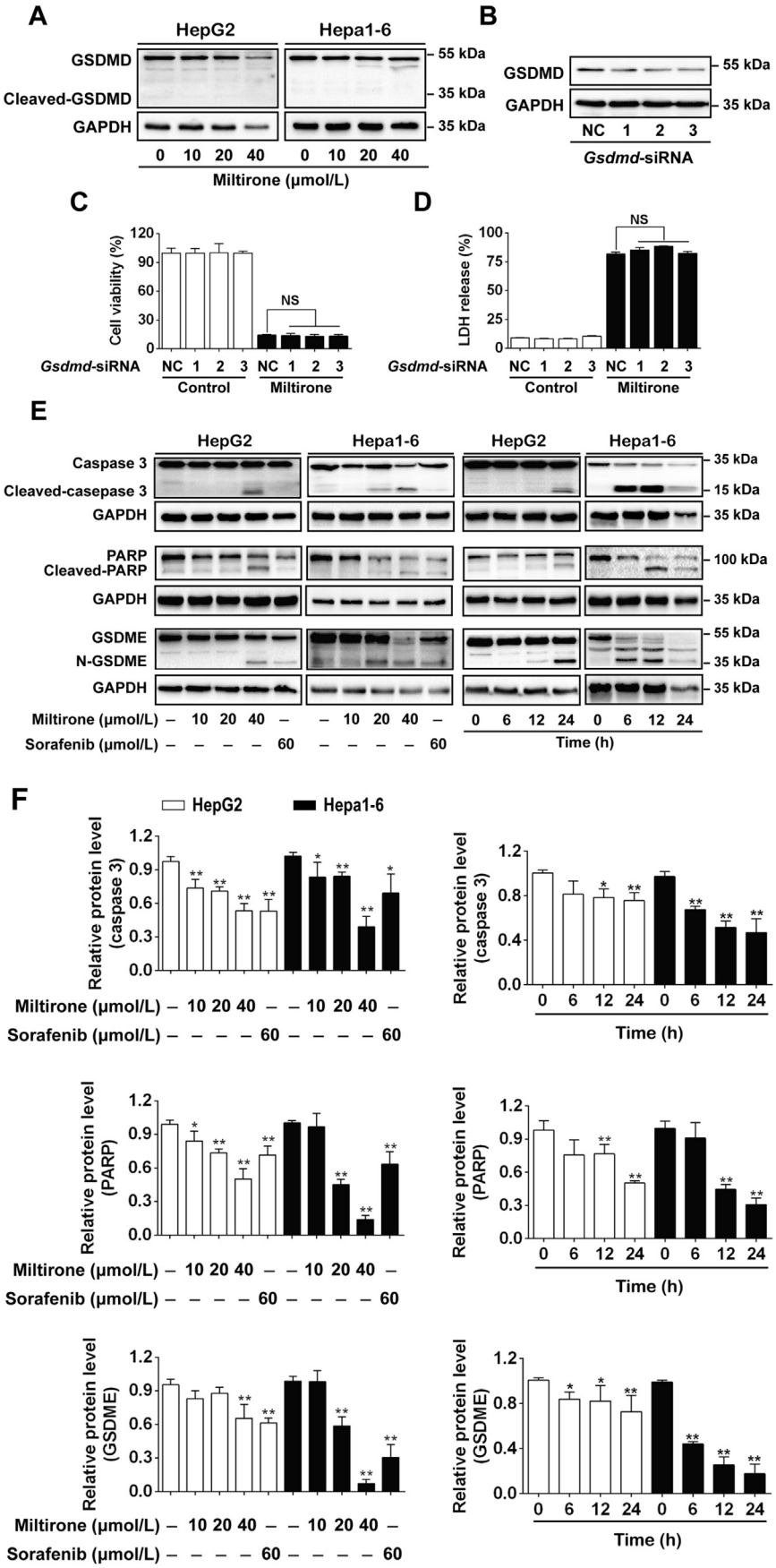
A
HepG2
Hepa1-6
GSDMD
Cleaved-GSDMD
GAPDH
55 kDa
35 kDa
35 kDa
0 10 20 40 0 10 20 40
Miltirone (μmol/L)
B
GSDMD
GAPDH
55 kDa
35 kDa
NC 1 2 3
Gsdmd-siRNA
C
Cell viability (%)
120
90
60
30
0
NS
Gsdmd-siRNA NC 1 2 3 NC 1 2 3
Control
Miltirone
D
LDH release (%)
100
75
50
25
0
NS
Gsdmd-siRNA NC 1 2 3 NC 1 2 3
Control
Miltirone
E
HepG2
Hepa1-6
HepG2
Hepa1-6
Caspase 3
Cleaved-casepase 3
GAPDH
35 kDa
15 kDa
35 kDa
PARP
Cleaved-PARP
GAPDH
100 kDa
35 kDa
GSDME
N-GSDME
GAPDH
55 kDa
35 kDa
35 kDa
Miltirone (μmol/L) – 10 20 40 – – 10 20 40 – 0 6 12 24 0 6 12 24
Sorafenib (μmol/L) – – – – 60 – – – – 60
Time (h)
F
HepG2
Hepa1-6
Relative protein level (caspase 3)
1.2
0.9
0.6
0.3
0.0
Miltirone (μmol/L) – 10 20 40 – – 10 20 40 –
Sorafenib (μmol/L) – – – – 60 – – – – 60
Relative protein level (caspase 3)
1.2
0.8
0.4
0.0
0 6 12 24 0 6 12 24
Time (h)
Relative protein level (PARP)
1.2
0.9
0.6
0.3
0.0
Miltirone (μmol/L) – 10 20 40 – – 10 20 40 –
Sorafenib (μmol/L) – – – – 60 – – – – 60
Relative protein level (PARP)
1.2
0.9
0.6
0.3
0.0
0 6 12 24 0 6 12 24
Time (h)
Relative protein level (GSDME)
1.2
0.9
0.6
0.3
0.0
Miltirone (μmol/L) – 10 20 40 – – 10 20 40 –
Sorafenib (μmol/L) – – – – 60 – – – – 60
Relative protein level (GSDME)
1.2
0.8
0.4
0.0
0 6 12 24 0 6 12 24
Time (h)

an absolute oral bioavailability of approximately 3.4%[24], we treated the mice with miltirone by intravenous injection *via* caudal vein. We performed the pilot experiments to determine the dosage of miltirone and found that miltirone significantly inhibited the growth of HCC solid tumors at a dose of 6 mg/kg (data not shown). Therefore, once the tumors volume reached an average of 100 mm^3, the mice were randomized into five groups ($n = 7$ in each group) and treated with either vehicle control [5% Tween-20, intravenous (i.v.)], lower dose of miltirone (1 mg/kg body weight, i.v.), middle dose of miltirone (3 mg/kg body weight, i.v.), or higher dose of miltirone (6 mg/kg body weight, i.v.) respectively once a day. As a positive control, mice were injected with sorafenib [10 mg/kg, intraperitoneal (i.p.)] once a day. The tumor volume (length × width × width × 3.14/6) and body weight of the mice were monitored every three days. At the end of treatment, mice were sacrificed and the tumors were removed, weighted, imaged, and analyzed *via* hematoxylin and eosin (H&E) staining and Western blotting. The animal experimental procedures complied with the guidelines for animal care of China Pharmaceutical University (Nanjing, China), and were approved by the Animal Ethics Committee of this institution (Nanjing, China).

2.12. Histopathologic examination

The tumor tissues, kidneys, and livers of mice were harvested and fixed in 4% paraformaldehyde, dehydrated, and embedded in paraffin. The paraffin-embedded tissue samples were sectioned into 5 μm slices and then stained with H&E. The histological features were observed and captured under a digital scanner (NanoZoomer 2.0, Hamamatsu, Japan).

2.13. Statistical analysis

Quantified results are shown as mean ± standard deviation (SD). Statistical analyses were performed with Prism six software (GraphPad). All *in vitro* experiments were performed at least three times. In all experiments, comparisons between two groups were tested for significance using the two-tailed Student's *t*-test. Statistical comparisons between three or more groups were performed using one-way analysis of variance (ANOVA) followed by Tukey multiple comparison. *P* values less than 0.05 were considered to be statistically significant.

3. Results

3.1. The effects of miltirone on HCC cells growth

To investigate the anti-cancer effects of miltirone in hepatocellular carcinoma, we used the HCC cells lines, HepG2 and Hepa1-6 (human and mouse, respectively), for our analyses. Sorafenib is a multi-kinase inhibitor that has shown efficacy against HCC[7]. As shown in Supporting Information Fig. S1, the cell viability of HCC cells (HepG2 and Hepa1-6) was substantial inhibited by treatment with sorafenib for 24 h in a dose-dependent manner. Based on these results, sorafenib (60 μmol/L) was used in the subsequent experiments as a positive control. To assess the effects of miltirone on HCC cells lines, the dose−response and time-course studies were performed in HepG2 and Hepa1-6 cells. Similar to the positive control, miltirone treatment dose-dependently inhibited HCC cells growth (Fig. 1B and C). The IC_{50} of miltirone for HepG2 and Hepa1-6 cells were 23.18 and 10.49 μmol/L, respectively (Supporting Information Table S1). Moreover, miltirone treatment significantly suppressed the cell viability of HepG2 or Hepa1-6 cells in a time-dependent manner (Fig. 1D). Collectively, these results suggested that miltirone inhibited the viability of either HepG2 or Hepa1-6 cells in dose- and time-dependent manners.

3.2. Miltirone changed cellular morphology and plasma membrane permeabilization

Firstly, the morphological changes were observed in HepG2 or Hepa1-6 cells upon miltirone or sorafenib exposure. As shown in Fig. 2A, miltirone-treated HepG2 and Hepa1-6 cells exhibited large bubbles emerging from the plasma membrane and cell swelling, which were distinct from classic apoptotic blebbing and reminiscent of characteristic pyroptotic cell morphology. Secondly, The HCC cells treated with miltirone displayed LDH release in a dose- and time-dependent manners, further indicating plasma membrane rupture and leakage (Fig. 2B and C). Confocal microscopy analysis demonstrated that miltirone treatment increased the percentage of PI-positive cells for HCC cells (HepG2 and Hepa1-6, respectively) in dose- and time-dependent manners (Fig. 2D and E). In the pyroptotic cells, pores can be formed in the cell membrane, permitting membrane impermeant dyes, such as PI, to enter into the cells and stain nuclei[25]. The increased LDH activities and PI-positive staining cells indicated that miltirone can change the plasma membrane permeability of HCC cells. Due to that cells undergoing necroptosis also showed membrane disruption, cell swelling, and lysis, the necroptosis inhibitor necrostatin-1 was used to distinguish pyroptosis from necroptosis[26]. As shown in Fig. 2F and G, necrostatin-1 had no significant effects on miltirone-induced cell death and LDH release. These data indicated that miltirone might trigger cell death by inducing plasma membrane permeabilization.

3.3. GSDME was essential for miltirone-induced pyroptosis in HCC cells

In gasdermin protein family members, GSDMD was identified as the substrate of caspase 1/4/5/11, and the cleavage of GSDMD can release the N-terminal domain of GSDMD to the membrane and

Figure 3 GSDMD is not involved in miltirone-induced cell death in HepG2 or Hepa1-6 cells. (A) HepG2 and Hepa1-6 cells were treated with miltirone (0−40 μmol/L) for 24 h, total cellular extracts were prepared and subjected to Western blotting analyses using antibodies against GSDMD and GADPH. (B) Hepa1-6 cells were transfected with siRNA targeting *Gsdmd* (*Gsdmd*-siRNA-1/2/3) or control siRNA (NC, negative control) for 24 h, total cellular extracts were prepared and subjected to Western blotting analyses using antibodies against GSDMD and GADPH ($n = 3$). (C) and (D) Hepa1-6 cells were transfected with siRNA targeting *Gsdmd* (*Gsdmd*-siRNA-1/2/3) or control siRNA (NC) for 24 h, cell viability was analyzed by CCK-8 assay, and LDH-release was analyzed using LDH assay kit and expressed as mean ± SD ($n = 3$). NS *vs.* NC. (E) and (F) HepG2 and Hepa1-6 cells were treated with miltirone (0−40 μmol/L) for 24 h, or treated with miltirone (40 μmol/L) for 6, 12, and 24 h, total cellular extracts were prepared and subjected to Western blotting analyses using antibodies against caspase 3, PARP, GSDME, and GADPH. Protein levels are expressed as mean ± SD ($n = 3$). $^{**}P < 0.05$, $^{**}P < 0.01$ *vs.* control.

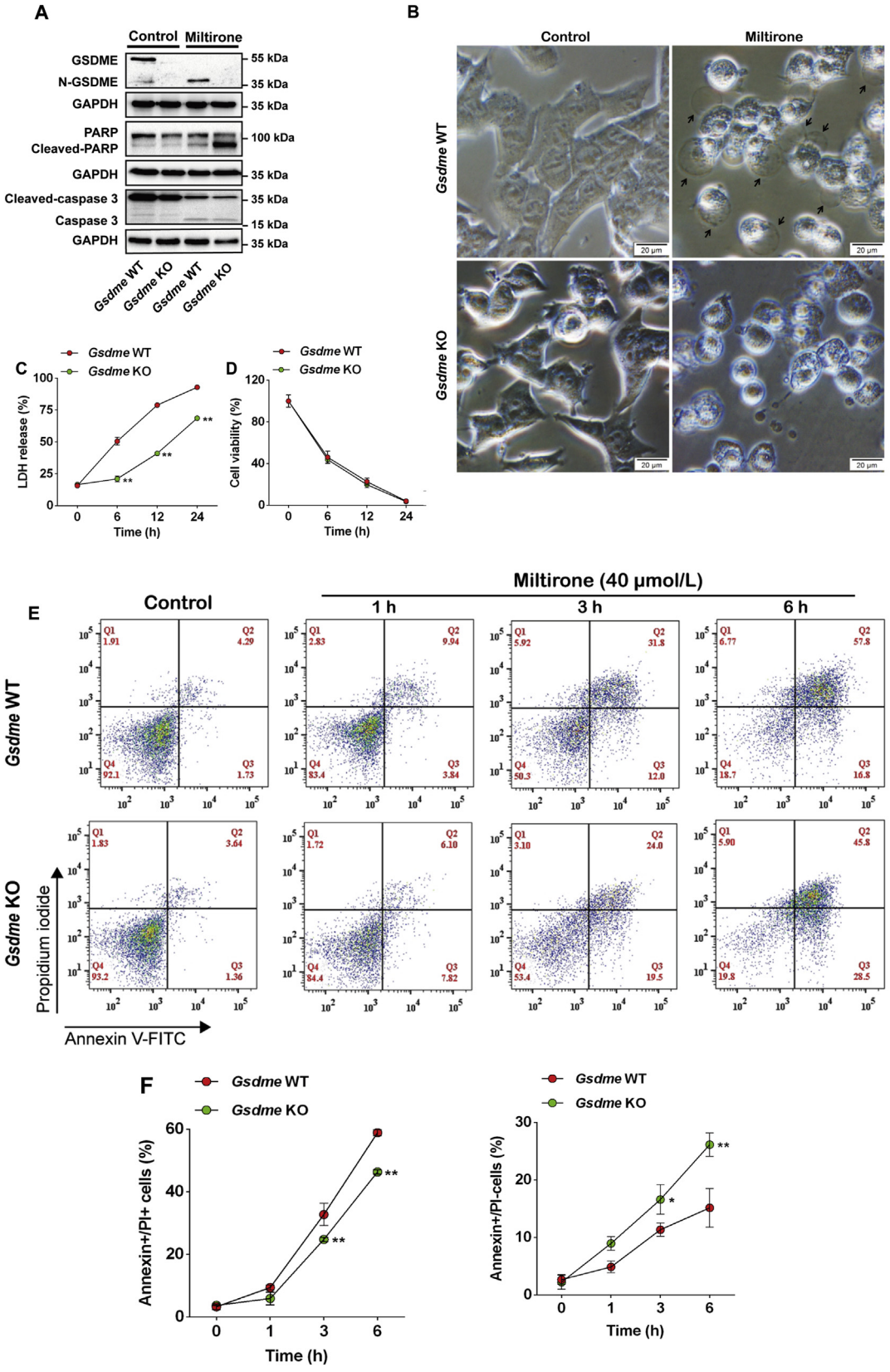

Figure 4 GSDME mediates pyroptosis in HCC cells in response to miltirone. (A) *Gsdme* wild-type (WT) and *Gsdme* KO Hepa1-6 cells were treated with miltirone (40 μmol/L) for 24 h, total cellular extracts were prepared and subjected to Western blotting analyses by using antibodies against caspase 3, PARP, GSDME, and GADPH ($n = 3$). (B) *Gsdme* WT and *Gsdme* KO Hepa1-6 cells were treated with miltirone (40 μmol/L) for 12 h, and microscopic imaging was performed. Arrowheads indicate ballooned cell membrane characteristic of pyroptotic cells, scale bar = 20 μm. (C) and (D) *Gsdme* WT and *Gsdme* KO Hepa1-6 cells were treated with miltirone (40 μmol/L) for 6, 12, and 24 h. Cell viability was analyzed by CCK-8 assay, and LDH-release was analyzed by LDH assay and expressed as mean ± SD ($n = 3$). $^{**}P < 0.01$ *vs.* GSDME WT. (E) and (F) *Gsdme* WT and *Gsdme* KO Hepa1-6 cells were treated with miltirone (40 μmol/L) for 1−6 h, stained by annexin V-FITC and PI, and analyzed by flow cytometry ($n = 3$). $^{*}P < 0.05$, $^{**}P < 0.01$ *vs. Gsdme* WT.

induce pyroptosis[27]. Although GSDMD were expressed in HepG2 and Hepa1-6 cells, miltirone treatment cannot induce the cleavage of GSDMD (Fig. 3A). Furthermore, knockdown of *Gsdmd* in Hepa1-6 (Fig. 3B) by siRNA did not affect miltirone-induced cell death and LDH release (Fig. 3C and D). Therefore, GSDMD is not involved in miltirone-induced cell death in HepG2 or Hepa1-6 cells.

GSDME, causally implicated in an autosomal-dominant heritable deafness, is a newly recognized effector of cell pyroptosis[15,28]. The previous report observed that no or little GSDME was expressed in several tumor types due to promoter hypermethylation[15]. Nevertheless, we found that GSDME were expressed in several HCC cell lines, which is consistent with the results from the Cancer Genome Atlas (TCGA) pan-cancergenomic interrogation (Supporting Information Fig. S2). Subsequent Western blotting analyses were performed and the results showed that miltirone induced cleavage of caspase three and PARP in HCC cells (HepG2 and Hepa1-6, respectively) in a dose-dependent manner (Fig. 3E and F). Importantly, miltirone treatment induced the release of N-terminal GSDME (N-GSDME), a marker of pyroptosis, in HepG2 or Hepa1-6 cells. These results are consistent with the pattern of caspase three cleavage (Fig. 3E and F). Miltirone treatment induced time-dependent cleavage of caspase 3, PARP, and GSDME in HCC cells (HepG2 and Hepa1-6, respectively, Fig. 3E and F). Then, we hypothesized that GSDME might be essential for miltirone-induced pyroptosis. To validate this hypothesis, we knocked out the *Gsdme* in Hepa1-6 cells using CRISPR-Cas9 technology (Fig. 4A). Genetic deletion of *Gsdme* resulted in significant reduction of miltirone-induced LDH release and plasma membrane ballooning, while did not rescued cell death in response to miltirone treatment (Fig. 4B−D). Miltirone-treated Hepa1-6 cells proceeded rapidly to the annexin V and PI double-positive stage, while KO of *Gsdme* delayed the process with increasing the proportion of annexin V single-positive cells and decreasing the percentage of double-positive cells (Fig. 4E and F). All these results suggested that the deficient of *Gsdme* might switch miltirone-induced cell death from pyroptosis to apoptosis. Western blotting analyses show that the cleavage of GSDME into N-GSDME was completely absent in *Gsdme* KO Hepa1-6 cells (Fig. 4A). Meanwhile, miltirone-treated *Gsdme* KO cells yielded more cleaved PARP (Fig. 4A), further confirming the apoptotic switch. Taken together, we concluded that GSDME is a key effector of miltirone-induced pyroptosis in HCC cells.

3.4. *Miltirone activated the mitochondrial intrinsic apoptotic pathway to elicit GSDME-dependent pyroptosis*

Recent findings have validated that GSDME-mediated pyroptosis can be triggered by the mitochondrial intrinsic apoptotic pathway[16,29]. Exposure of Hepa1-6 cells to miltirone caused disruption of MMP as evidenced by an increase in the proportion of cells with green fluorescence and a decrease in the proportion of cells with red JC-1 fluorescence (Supporting Information Fig. S3A). We also examined the level of caspases in response to miltirone by Western blotting. As expected, miltirone effectively increased the protein levels of BAX and cleaved-caspase nine in dose-dependent manners, indicating that the miltirone-induced pyroptosis in Hepa1-6 cells might be mediated through caspase pathway (Figs. S3B and S3C). Then, combined treatment with miltirone and the caspase 3-specific inhibitor, Z-DEVD-FMK, considerably decreased proteolytic cleavage of GSDME and extracellular release of LDH (Fig. 5A and B). Additionally, the siRNA technology was employed to verify whether caspase three is involved in pyroptosis induction. In Hepa1-6 cells, three siRNA duplexes against caspase three were evaluated, whereas the expressions of caspase three were weakly inhibited. Nonetheless, knockdown of caspase three resulted in the visible decrease of N-GSDME generation (Fig. 5C), LDH release (Fig. 5D), and the percentage of annexin V-PI double positive cells (Fig. 5E). These results demonstrated that miltirone induced GSDME-dependent pyroptosis in HCC cells by activating the mitochondrial intrinsic apoptotic pathway.

3.5. *Miltirone inhibited MEK/ERK1/2 signaling pathway for pyroptosis induction*

The phosphatidylinositol 3-kinase (PI3K)/AKT serine/threonine kinase (AKT)/mammalian target of rapamycin (mTOR) and the RAF/MEK/ERK1/2 signaling pathways are critical for several cancer development and progression, including HCC[30,31]. Recent studies have established that activated AKT and ERK1/2 are associated with frequent intrahepatic metastasis and vascular invasion, advanced tumor stage, and high proliferation index in HCC[32−34]. As compared with the control, the protein levels of AKT and phosphorylated-AKT (p-AKT) were no significant change in miltirone-treated Hepa1-6 cells (Fig. 6A). The total protein levels of MEK and ERK1/2 showed no obvious changes, but phosphorylated levels of MEK and ERK1/2 decreased in response to miltirone treatment (Fig. 6B and C). Remarkably, ERK1/2 activator, ceramide C6 (Santa Cruz Biotechnology), effectively reduced the release of LDH and inhibited the cleavage of GSDME and caspase 3 (Fig. 6D−F). Therefore, we deduced that miltirone-induced pyroptosis in HCC cells was mediated through MEK/ERK1/2 signaling pathway.

3.6. *Miltirone induced pyroptosis through ROS mediated damage in HCC cells*

Miltirone has been reported to induce HCC cells apoptosis by activating the ROS-dependent mitochondrial intrinsic apoptotic pathway[22]. However, whether miltirone-elevated ROS is associated to pyroptosis is currently unknown. We first performed confocal microscopy and flow cytometry to determine the intracellular ROS accumulation. Flow cytometric and confocal microscopic analyses illustrated that miltirone treatment triggered overproduction of ROS in Hepa1-6 cells, and this effect was markedly abrogated by the ROS scavenger NAC (Fig. 7A and Supporting Information Fig. S4). The level of ROS did not change obviously in sorafenib group (Fig. S4). To evaluate the role of ROS in miltirone-induced pyroptosis in HCC cells, the NAC pretreated Hepa1-6 cells were stimulated with miltirone and the cell viability was assessed. The results showed that NAC can rescue miltirone-induced cell death (Fig. 7B). Moreover, combined treatment with miltirone and NAC reversed the release of LDH, activation of BAX, and cleavage of caspase 9, caspase 3, and GSDME (Fig. 7C−G).

It has been reported that MEK/ERK1/2 is the downstream signal transducers involved in the activation of ROS-mediated cascades[31]. We sought to elucidate how ROS and MEK/ERK1/2 signal pathway participated in the miltirone-induced pyroptosis. In Hepa1-6 cells, miltirone treatment decreased both p-MEK and p-ERK1/2 protein levels, while combined treatment with NAC can

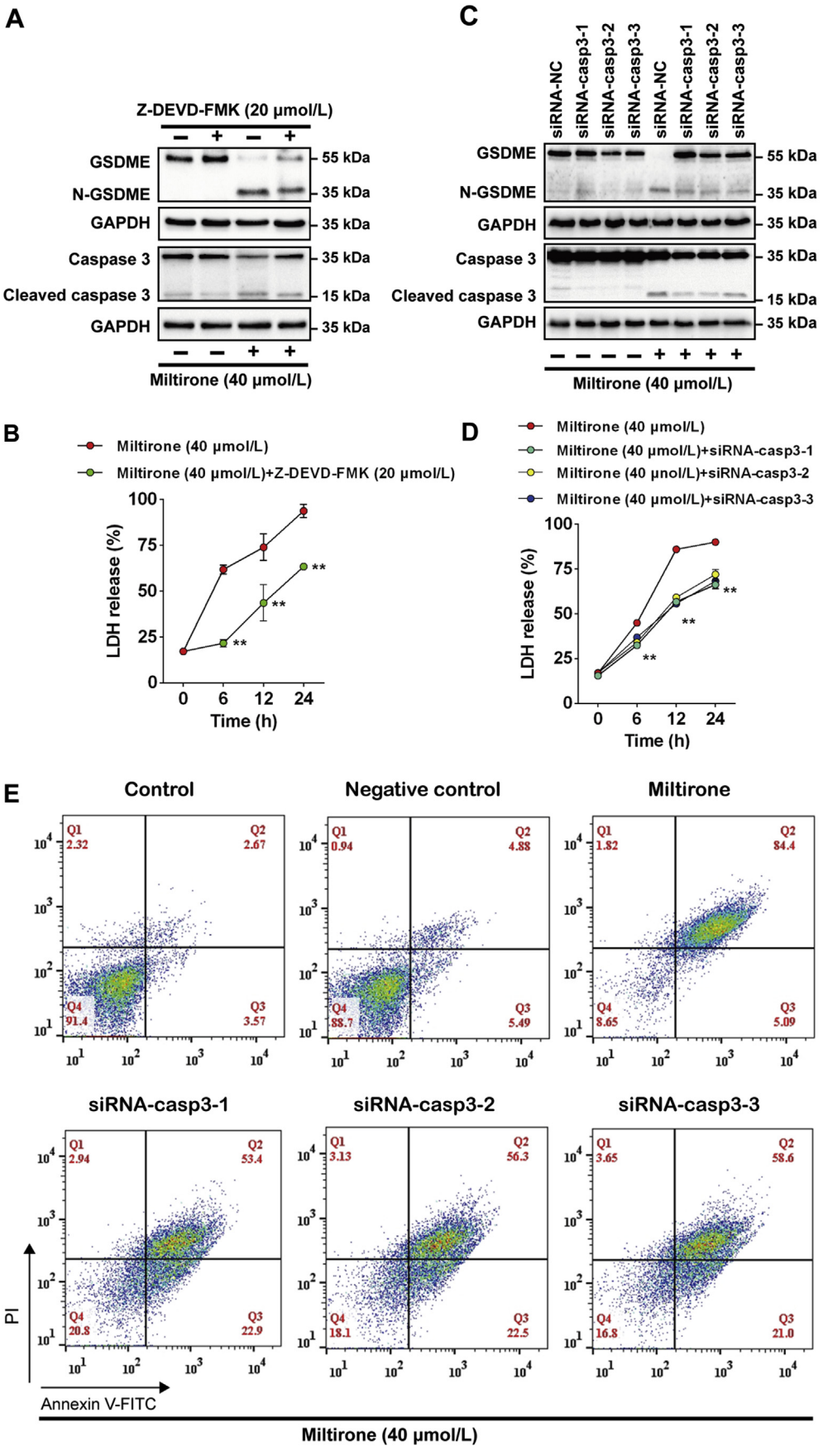
A
Z-DEVD-FMK (20 μmol/L)
GSDME
N-GSDME
GAPDH
Caspase 3
Cleaved caspase 3
GAPDH
55 kDa
35 kDa
35 kDa
35 kDa
15 kDa
35 kDa
Miltirone (40 μmol/L)
C
siRNA-NC
siRNA-casp3-1
siRNA-casp3-2
siRNA-casp3-3
Miltirone (40 μmol/L)
B
Miltirone (40 μmol/L)
Miltirone (40 μmol/L)+Z-DEVD-FMK (20 μmol/L)
LDH release (%)
Time (h)
D
Miltirone (40 μmol/L)
Miltirone (40 μmol/L)+siRNA-casp3-1
Miltirone (40 μnol/L)+siRNA-casp3-2
Miltirone (40 μmol/L)+siRNA-casp3-3
E
Control
Negative control
Miltirone
siRNA-casp3-1
siRNA-casp3-2
siRNA-casp3-3
PI
Annexin V-FITC
Miltirone (40 μmol/L)

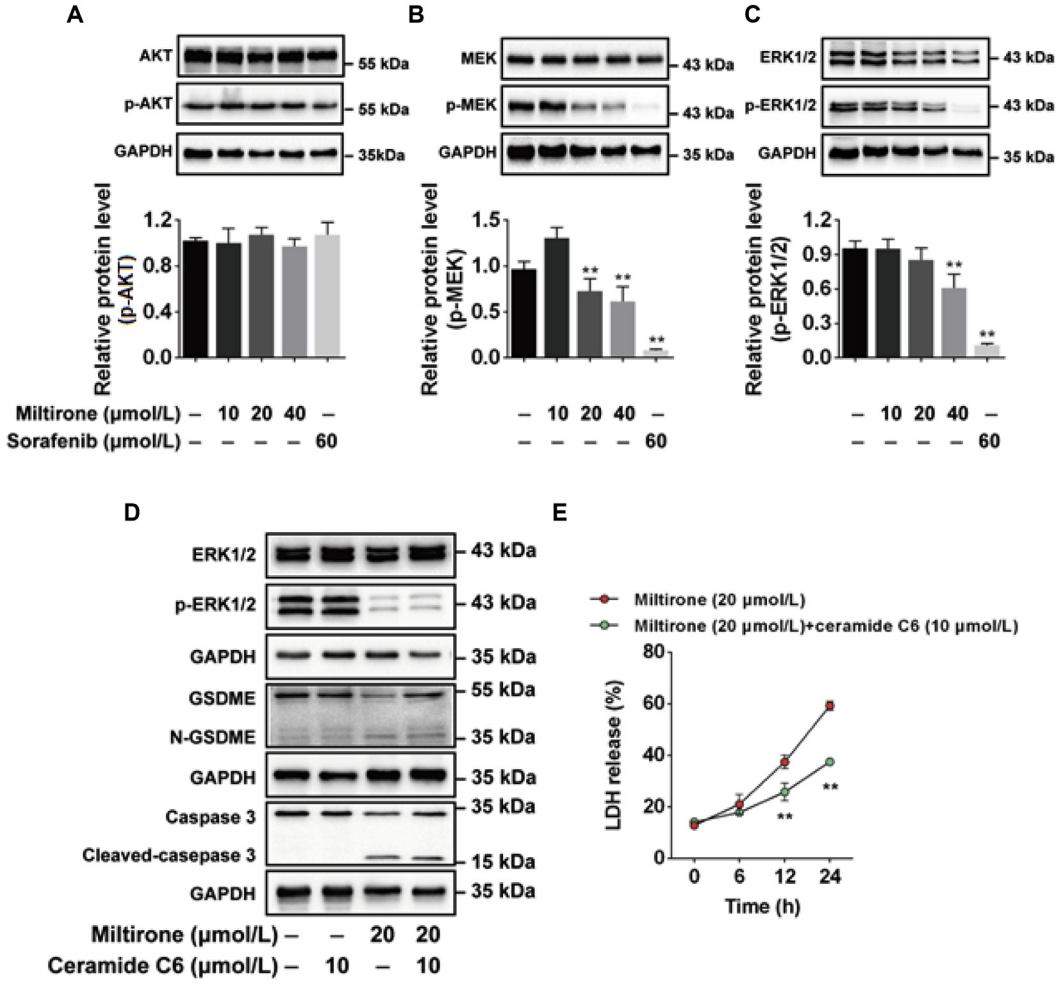

Figure 6 Miltirone induced HCC cells pyroptosis is mediated through RAF/MEK/ERK1/2 signaling pathway. (A)−(C) Hepa1-6 cells were treated with miltirone (0−40 μmol/L) for 24 h, total cellular extracts were prepared and subjected to Western blotting analyses using AKT, p-AKT, MEK, p-MEK, ERK1/2, p-ERK1/2, and GADPH antibodies. Protein levels were expressed as mean ± SD ($n = 3$). (D) Hepa1-6 cells were treated with miltirone (20 μmol/L) in the absence or presence of ceramide C6 (10 μmol/L) for 6, 12, and 24 h, LDH release were measured by LDH assay and expressed as mean ± SD ($n = 3$). $^{*}P < 0.05$, $^{**}P < 0.01$, *vs.* miltirone alone at each indicated time. (E) Hepa1-6 cells were treated with miltirone (20 μmol/L) in the absence or presence of ceramide C6 (10 μmol/L) for 24 h, total cellular extracts were prepared and subjected to Western blotting analyses using antibodies against ERK1/2, p-ERK1/2, caspase 3, GSDME, and GADPH ($n = 3$).

reverse these changes (Fig. 7H−I). Overall, these data revealed that ROS, as a negative regulator of MEK/ERK1/2, played an essential role in miltirone-induced pyroptosis.

3.7. Miltirone inhibited the tumor growth and induced HCC cells pyroptosis in vivo

Using the Hepa1-6 mouse HCC syngeneic model, the anti-HCC activity of miltirone was tested *in vivo*. As a positive control, tumor growth was strongly inhibited by sorafenib, which was consistent with the previous studies[7]. Miltirone at all three doses significantly inhibited the growth of HCC solid tumors (on Day 27). The effects of miltirone at the high dose (6 mg/kg) on tumor volume and weight were comparable to those of sorafenib (Fig. 8A). The average of tumor weight decreased from 812.1 mg (vehicle) to 451.3 mg (miltirone at 1 mg/kg dose), 338.4 mg (miltirone at 3 mg/kg dose), 188.3 mg (miltirone at 6 mg/kg dose), and 142.8 mg (sorafenib at 10 mg/kg dose), respectively (Fig. 8B).

Figure 5 Miltirone activates the mitochondrial intrinsic apoptotic pathway to elicit GSDME-dependent pyroptosis. (A) Hepa1-6 cells were treated with miltirone (40 μmol/L) in the absence or presence of Z-DEVD-FMK (20 μmol/L) for 24 h, total cellular extracts were prepared and subjected to Western blotting analyses using antibodies against caspase 3, GSDME, and GADPH ($n = 3$). (B) Hepa1-6 cells were treated with miltirone (40 μmol/L) in the absence or presence of Z-DEVD-FMK (20 μmol/L) for 6, 12, and 24 h, LDH-release was analyzed using LDH assay kit and expressed as mean ± SD ($n = 3$). $^{**}P < 0.01$, *vs.* miltirone alone at each indicated time. Hepa1-6 cells were transfected with siRNA targeting caspase 3 (siRNA-casp3-1/2/3) or control siRNA and then treated with miltirone for 24 h. (C) Total cellular extracts were prepared and subjected to Western blotting analyses using antibodies against caspase 3, GSDME, and GADPH ($n = 3$). (D) LDH-release was analyzed by LDH assay and expressed as mean ± SD ($n = 3$). $^{**}P < 0.01$, *vs.* miltirone alone at each indicated time. (E) Annexin V-FITC and PI stained cells were analyzed by flow cytometry.

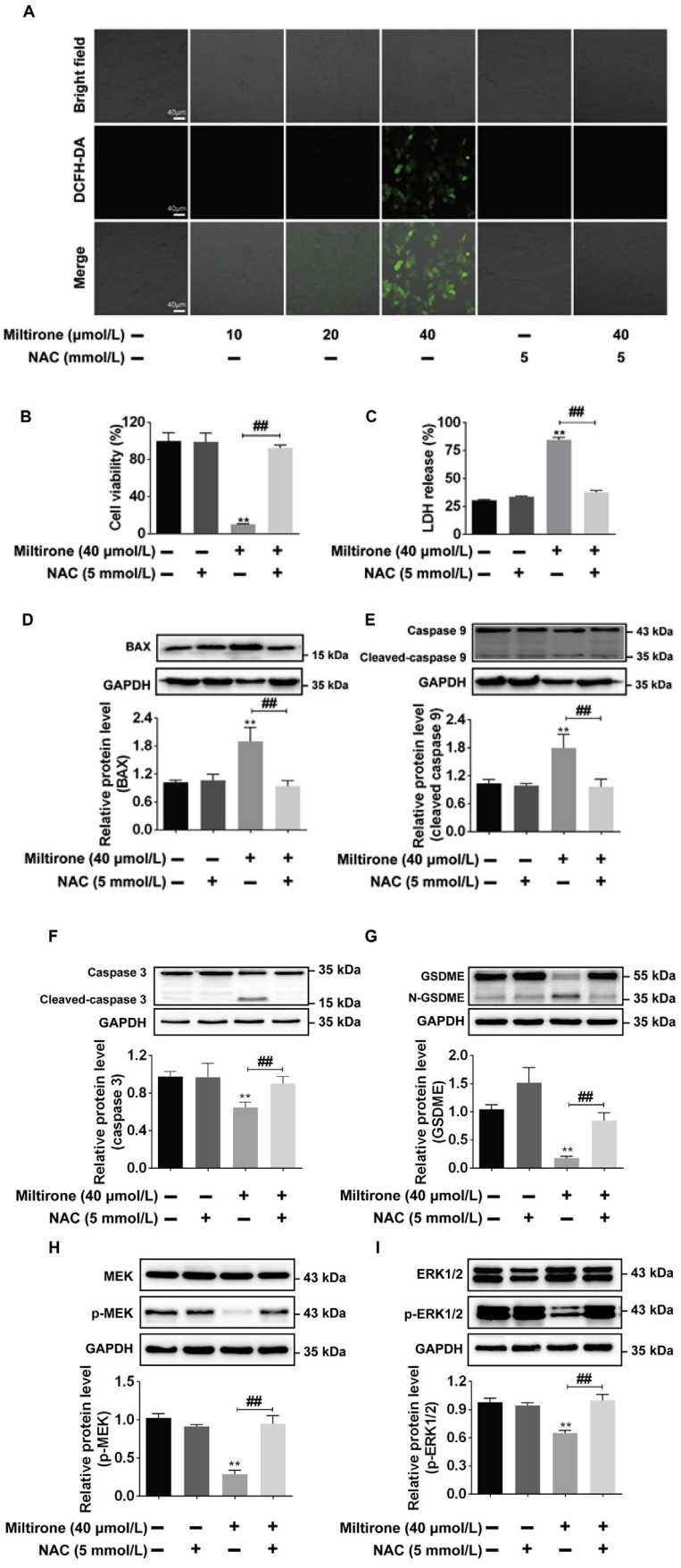
A
Bright field
DCFH-DA
Merge
40μm
Miltirone (μmol/L) — 10 20 40 — 40
NAC (mmol/L) — — — — 5 5
B
Cell viability (%)
120
80
40
0
##
**
Miltirone (40 μmol/L) — — + +
NAC (5 mmol/L) — + — +
C
LDH release (%)
100
75
50
25
0
##
**
Miltirone (40 μmol/L) — — + +
NAC (5 mmol/L) — + — +
D
BAX
15 kDa
GAPDH
35 kDa
Relative protein level (BAX)
2.4
1.8
1.2
0.6
0.0
##
**
Miltirone (40 μmol/L) — — + +
NAC (5 mmol/L) — + — +
E
Caspase 9
43 kDa
Cleaved-caspase 9
35 kDa
GAPDH
35 kDa
Relative protein level (cleaved caspase 9)
2.4
1.8
1.2
0.6
0.0
##
**
Miltirone (40 μmol/L) — — + +
NAC (5 mmol/L) — + — +
F
Caspase 3
35 kDa
Cleaved-caspase 3
15 kDa
GAPDH
35 kDa
Relative protein level (caspase 3)
1.2
0.8
0.4
0.0
##
**
Miltirone (40 μmol/L) — — + +
NAC (5 mmol/L) — + — +
G
GSDME
55 kDa
N-GSDME
35 kDa
GAPDH
35 kDa
Relative protein level (GSDME)
2.0
1.5
1.0
0.5
0.0
##
**
Miltirone (40 μmol/L) — — + +
NAC (5 mmol/L) — + — +
H
MEK
43 kDa
p-MEK
43 kDa
GAPDH
35 kDa
Relative protein level (p-MEK)
1.5
1.0
0.5
0.0
##
**
Miltirone (40 μmol/L) — — + +
NAC (5 mmol/L) — + — +
I
ERK1/2
43 kDa
p-ERK1/2
43 kDa
GAPDH
35 kDa
Relative protein level (p-ERK1/2)
1.2
0.9
0.6
0.3
0.0
##
**
Miltirone (40 μmol/L) — — + +
NAC (5 mmol/L) — + — +

Images of the tumors confirmed the efficacy of miltirone in reducing tumor burden in the HCC model (Fig. 8C). Histological assessment of tumors from vehicle-treated animals shows loss of architecture and presence of hyper chromatin and hypercellularity. Treatment with miltirone at the high dose (6 mg/kg) resulted in obvious cell cavitation and condensed chromatin in tumor tissues (Fig. 8H). The average body weight of miltirone-treated mice did not significantly decrease as compared with that of the control mice (Fig. 8D). In addition, no morphological changes were observed in the kidneys and livers of the miltirone-treated mice, suggesting miltirone had no significant toxicity to the mice (Fig. 8H).

Additionally, we examined whether reduction of tumor volume was associated with miltirone-induced pyroptosis. The level of serum LDH is increased in either miltirone or sorafenib treatment group as compared with vehicle group (Fig. 8E). Moreover, we analyzed the protein levels of pyroptosis-related factors in tumor tissues. The results show that miltirone treatment upregulated the protein levels of N-GSDME and cleaved-caspase three in a dose-dependent manner (Fig. 8F and G). Collectively, these results suggest that miltirone might inhibit the growth of HCC tumors *in vivo* by inducing pyroptosis.

4. Discussion

This study demonstrated that miltirone, a potential anti-cancer agent isolated from *S. miltiorrhiza*, significantly suppressed HCC *in vitro* and *in vivo* by inducing pyroptosis. We further investigated the underlying molecular mechanism and revealed that the pro-pyroptosis activity of miltirone was associated with its ability to stimulate ROS production, suppress MEK/ERK1/2 activation, and activate mitochondrial intrinsic apoptotic pathway.

HCC represents a common international health problem. Despite improved surveillance programs globally achieved, the overall 5-year survival remains poor (20%)[35,36]. Chemotherapy remains the mainstay of treatment for advanced HCC[37,38]. Sorafenib is the standard therapy for patients with advanced HCC, but it only provides limited survival benefit for patients[8,39]. Therefore, there is an urgency to identify more promising agents of high curative value as well as low toxicity for HCC therapy. Cell viability assay demonstrated that miltirone can inhibit the growth of HepG2 or Hepa1-6 cells. Additionally, *in vivo* experimental HCC model revealed that treatment with miltirone significantly inhibited the HCC tumor growth. Our data concur with previous reports about the therapeutic potential of miltirone in cancer treatment[18−22].

Apoptosis was generally considered as the predominant form of regulated cell death responsible for tumor therapies, a notion that was widely reported by numerous studies[40,41]. Miltirone used for cancer therapy attributed to its ability to inhibit cancer cell growth and to induce cancer cell apoptosis[19−21]. Zhou et al.[22] has demonstrated the apoptotic induction activity of miltirone in HepG2. In this present study, we expanded the conventional view, and proposed the GSDME-dependent pyroptosis was involved in the therapy of miltirone in HCC, as supported by the following evidence. Firstly, our results showed that the hallmark features of pyroptosis, such as GSDME cleavage, balloon-like bubbles, LDH release, and PI-positive staining, were observed in miltirone-treated HCC cells. It should be noted that cells undergoing necroptosis also exhibit plasma membrane permeabilization, cell swelling, and lysis[26]. Necrostatin-1, an inhibitor of necroptosis, had no significant effects on cell viability and LDH release. It was suggested that cell death triggered by miltirone in our study was not necroptosis. Secondly, we compared the GSDME protein expression in five HCC cell lines with human liver cells (L02), and confirmed that GSDME was commonly expressed in HCC cell lines. During pyroptosis, pores open in the cell membrane, permitting annexin V to enter the cells and stain the inner leaflets of the membrane. In contrast, membrane impermeant dyes, such as 7-aminoactinomycin D (7-AAD) or PI, stain pyroptotic cells by entering through the pores, but do not stain apoptotic cells[25,42]. We found that miltirone-treated Hepa1-6 cells proceeded directly to the annexin V and PI double-positive stage, while KO of *Gsdme* delayed the process with increasing the proportion of annexin V single-positive cells and decreasing the percentage of double-positive cells. *Gsdme* KO did not rescue cell death in response to miltirone treatment, whereas resulted in reduction of miltirone-induced LDH release and plasma membrane ballooning, further confirming pyroptosis to apoptosis switch. Activated GSDMD protein is also found to determine pyroptosis[13]. But, knockdown of *Gsdmd* in Hepa1-6 by siRNA did not affect the miltirone-induced cell death and LDH release. Although GSDMD was expressed in HCC cells, miltirone-treatment did not induce the cleavage of GSDMD. Therefore, GSDMD is not involved in miltirone-induced pyroptosis in HCC cells. Thirdly, the GSDME-dependent pyroptotic cell death can be triggered by the mitochondrial apoptotic signaling[16,29,43]. Consistently, our findings showed that miltirone induced mitochondrial depolarization and dose-dependently increased the protein levels of BAX, cleaved-caspase 9, cleaved-caspase 3, and N-GSDME in Hepa1-6 cells. In contrast, the siRNA of caspase three and the caspase 3-specific inhibitor Z-DEVD-FMK inhibited miltirone-induced pyroptosis, suggesting that the activation of mitochondria-mediated caspases was required for miltirone-induced pyroptosis in HCC cells. Lastly, *in vivo* evidences further demonstrated that miltirone induced tumor cell pyroptosis in HCC tumors.

The preliminary observation of signaling interrelation between pyroptosis and apoptosis suggests that the two death modes may reciprocally regulate each other to produce cytotoxic inhibition. While, there exists great divergence about how tumor cell apoptosis and pyroptosis were co-opted and orchestrated in the context of chemotherapy. Yu et al.[43] demonstrated that two forms of regulated cell death may exist simultaneously upon chemotherapy drugs exposure. Consistent with this previous study, our results indicated that the biochemical markers for apoptosis and pyroptosis were invariably synchronously detected in miltirone-stimulated HCC cells. We also supported that a conceivable interplay between cell pyroptosis and apoptosis might exist and substrates cleaved by caspases in a cellular context were

Figure 7 ROS−MEK/ERK1/2 signaling pathway participates in miltirone-induced pyroptosis in HCC cells. (A) Hepa1-6 cells were treated with miltirone and/or NAC for 2 h, intracellular ROS content was measured with confocal microscopy. Scale bar = 40 μm Hepa1-6 cells were treated with miltirone and/or NAC for 24 h. (B) and (C) Cell viability and LDH release were measured, respectively, and expressed as mean ± SD ($n = 3$). (D)−(I) Total cellular extracts were prepared and subjected to Western blotting analyses using antibodies against BAX, caspase 9, caspase 3, GSDME, MEK, p-MEK, ERK1/2, p-ERK1/2, and GADPH. $^{**}P < 0.01$ *vs.* control; $^{\#\#}P < 0.01$, *vs.* miltirone alone.

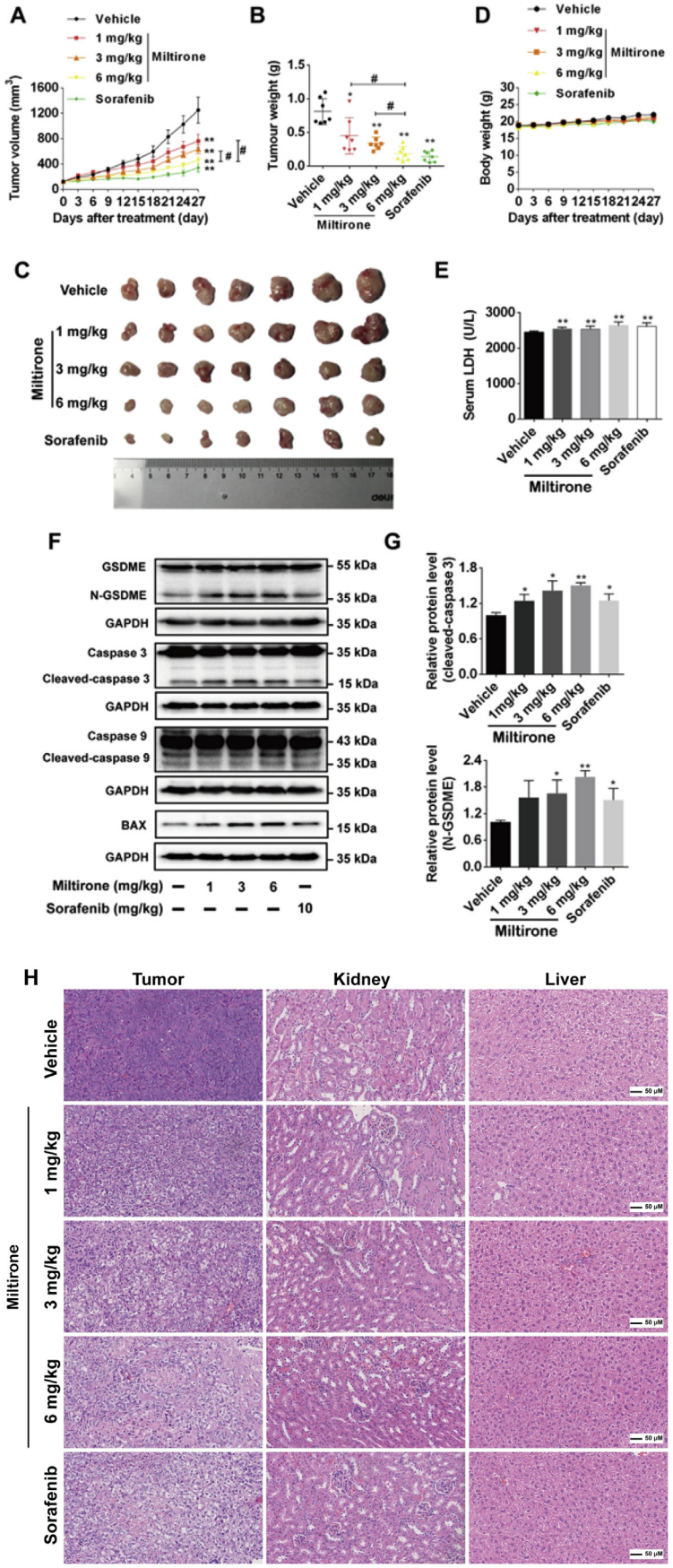
A
Vehicle
1 mg/kg
3 mg/kg
6 mg/kg
Miltirone
Sorafenib
Tumor volume (mm3)
Days after treatment (day)
B
Tumour weight (g)
Vehicle
1 mg/kg
3 mg/kg
6 mg/kg
Sorafenib
Miltirone
D
Body weight (g)
Days after treatment (day)
C
Vehicle
1 mg/kg
3 mg/kg
6 mg/kg
Miltirone
Sorafenib
E
Serum LDH (U/L)
F
GSDME
N-GSDME
GAPDH
Caspase 3
Cleaved-caspase 3
Caspase 9
Cleaved-caspase 9
BAX
55 kDa
35 kDa
15 kDa
43 kDa
Miltirone (mg/kg)
Sorafenib (mg/kg)
G
Relative protein level (cleaved-caspase 3)
Relative protein level (N-GSDME)
H
Tumor
Kidney
Liver
Vehicle
1 mg/kg
3 mg/kg
6 mg/kg
Miltirone
Sorafenib

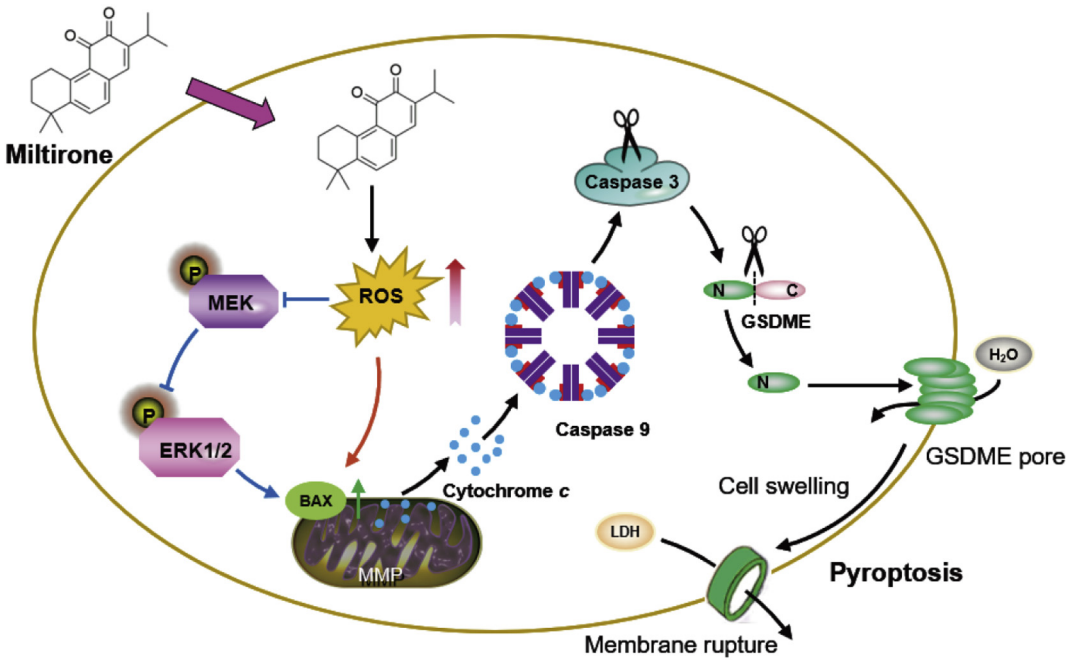

Figure 9 A schematic summary of this study, showing that through regulating ROS/ERK1/2 pathway, miltirone can elicit BAX−caspase−GSDME-dependent pyroptosis.

responsible for the type of cell death[29]. Knocking out *Gsdme* switches miltirone-induced cell death from pyroptosis to apoptosis, reinforces the point that therapy-induced pyroptosis might precede apoptosis. Moreover, GSDME has been reported to augment caspase 3/7 activation and apoptotic cell death by targeting the mitochondria[44]. Cleavage of GSDME by death receptor signaling bridges the extrinsic to the intrinsic apoptotic pathway[44]. Considering of these results, we proposed that the signaling crosstalk between pyroptosis and apoptosis may have implication in determining the type of cell death.

RAF/MEK/ERK1/2 signaling pathway exerts a core role in regulating cancer cell proliferation, differentiation, and survival[7,32]. Activation of the RAF/MEK/ERK1/2 signaling pathway was detected in up to 58% of all HCC samples analyzed[45−47]. A scintillation proximity assay for the high-throughput screening and identification of selective RAF/MEK/ERK1/2 enzyme inhibitors had already been developed[48]. And as the first oral multi-kinase inhibitor that targets RAF/MEK/ERK1/2 pathway, sorafenib has been discovered and approved for advanced hepatocellular carcinoma[6]. Miltirone was previously reported to induce HCC cells apoptosis by inhibiting the phosphorylation of ERK1/2[22]. However, whether RAF/MEK/ERK1/2 signaling pathway is involved in the miltirone-induced pyroptosis remains unclear. In this present study, we found that miltirone treatment significantly inhibited the phosphorylation of MEK and ERK1/2 in Hepa1-6 cells. Moreover, ceramide C6 (an ERK1/2 activator) inhibited the miltirone-induced pyroptosis in Hepa1-6 cells, as indicated by the LDH assay. These data suggest that, at least partially, MEK/ERK1/2 signaling is involved in the miltirone-induced pyroptosis. RAF/MEK/ERK1/2 pathway is associated with the intrinsic apoptotic pathway characterized by overexpression of BAX, release of cytochrome c from mitochondria and activation of caspase 3[49−51]. Indeed, inhibited RAF/MEK/ERK1/2 signaling pathway induced activation of BAX and cleavage of caspase 9, caspase 3, and GSDME in Hepa1-6 cells. Thus, it was suggested that MEK/ERK1/2 was likely an upstream regulator of caspase-mediated GSDME activation. While, whether the suppression of MEK/ERK1/2 signaling is directly related to caspase activation needs to be further investigated.

Previous studies have shown that ROS induced by miltirone is essential for its therapeutic effect on HCC[22,31]. Excessive accumulation of ROS can cause the oxidation and oligomerization of the mitochondrial outer membrane protein Tom20. BAX is recruited to mitochondria by oxidized Tom20, which facilitates the cytochrome c release to cytosol to activate caspase 3, eventually triggering pyroptotic death by inducing GSDME cleavage[52]. Consistently, we proved that miltirone administration could

Figure 8 Miltirone inhibits the tumor growth and induces HCC cells pyroptosis *in vivo*. Hepa1-6 cells were inoculated into mice to establish tumor model as described in the Material and methods. Mice bearing tumors were randomly grouped and administered vehicle (Vehicle), 1 mg/kg body weight of miltirone (1 mg/kg), 3 mg/kg body weight of miltirone (3 mg/kg), 6 mg/kg body weight of miltirone (6 mg/kg), or 10 mg/kg weight of sorafenib (Sorafenib), respectively. (A) The tumor volume measurement was proceeded every other day, presented as mean ± standard error of mean (SEM), $n = 7$. (B) The tumors were dissected and weighted (presented as mean ± SD, $n = 7$). (C) Representative photographs of isolated tumors at Day 27 after treatment. (D) Body weight of mice during the 27 days (presented as mean ± SD, $n = 7$). (E) The release of serum LDH in the mice was measured by LDH assay (presented as mean ± SD, $n = 7$). (F) and (G) Western blotting analyses of GSDME, N-GSDME, caspase 3, cleaved-caspase 3, caspase 9, cleaved-caspase 9, and BAX expression in treated tumor tissues. Protein levels were expressed as mean ± SD ($n = 3$). (H) Histological analysis of tumors, kidneys, and livers at the end of experiment. Scale bar = 50 μm. $^{*}P < 0.05$, $^{**}P < 0.01$ *vs.* vehicle treatment; $^{\#}P < 0.05$ *vs.* indicated treatment.

lead to the elevation of ROS, which in turn causing BAX−caspase−GSDME mediated pyroptosis in HCC cells. On the other hand, we also demonstrated that NAC, a ROS scavenger, reversed the miltirone-induced pyroptosis induction and suppression of p-ERK1/2 in Hepa1-6 cells. However, ROS generation was not significantly affected by the MEK/ERK1/2 pathway inhibitor, implying that ROS is a regulator of MEK/ERK1/2 signaling. Moreover, it was demonstrated that miltirone inhibited MEK/ERK1/2 signaling pathway for pyroptosis induction. These evidences suggested that miltirone induced pyroptosis through BAX−caspase−GSDME pathway in HCC cells *via* the ROS/MEK/ERK1/2 signaling.

5. Conclusions

Our results demonstrated that miltirone might be a potential candidate agent for the treatment of HCC. We further investigated the mechanism of these effects, and indicated that a central signaling axis, ROS/ERK1/2−BAX−caspase 9−caspase 3−GSDME, was demonstrated to regulate the miltirone-induced pyroptotic process (Fig. 9). These findings provide a new insight that GSDME-dependent pyroptosis is an unrecognized mechanism by which miltirone exerts therapeutic action.

Acknowledgments

This work was financially supported by National Key R&D Program of China (No. 2018YFC1704500) and "Double First-Class" University Project (No. CPU2018GY03, China).

Author contributions

Xiaowei Zhang conceived the experiments, performed the majority of experiments, analyzed the data, and drafted the paper. Ping Zhang, Lin An, Ningyuan Sun, Liying Peng, and Weiwei Tang performed partial experiments and acquired the data. Jun Chen designed the study, supervised the experiments, and gave the final approval of the manuscript. Dingyuan Ma designed the study, analyzed the data, wrote a part of the paper, and revised the paper. All authors read and approved the manuscript as submitted.

Conflicts of interest

The authors declare no conflicts of interest.

Appendix A. Supporting information

Supporting data to this article can be found online at https://doi.org/10.1016/j.apsb.2020.06.015.

References

1. Bray F, Ferlay J, Soerjomataram I, Siegel RL, Torre LA, Jemal A. Global cancer statistics 2018: GLOBOCAN estimates of incidence and mortality worldwide for 36 cancers in 185 countries. *CA Cancer J Clin* 2018;**68**:394−424.
2. Keating GM, Santoro A. Sorafenib: a review of its use in advanced hepatocellular carcinoma. *Drugs* 2009;**69**:223−40.
3. Augello G, Emma MR, Cusimano A, Azzolina A, Mongiovì S, Puleio R, et al. Targeting HSP90 with the small molecule inhibitor AUY922 (luminespib) as a treatment strategy against hepatocellular carcinoma. *Int J Canc* 2019;**144**:2613−24.
4. Llovet JM, Ricci S, Mazzaferro V, Hilgard P, Gane E, Blanc JF, et al. Sorafenib in advanced hepatocellular carcinoma. *N Engl J Med* 2008;**359**:378−90.
5. Cheng AL, Kang YK, Chen ZD, Tsao CJ, Qin SK, Kim JS, et al. Efficacy and safety of sorafenib in patients in the Asia-Pacific region with advanced hepatocellular carcinoma: a phase III randomized, double-blind, placebo-controlled trial. *Lancet Oncol* 2009;**10**:25−34.
6. Wilhelm S, Carter C, Lynch M, Lowinger T, Dumas J, Smith RA, et al. Discovery and development of sorafenib: a multikinase inhibitor for treating cancer. *Nat Rev Drug Discov* 2006;**5**:835−44.
7. Liu L, Cao YC, Chen C, Zhang XM, McNabola A, Wilkie D, et al. Sorafenib blocks the RAF/MEK/ERK pathway, inhibits tumor angiogenesis, and induces tumor cell apoptosis in hepatocellular carcinoma model PLC/PRF/5. *Cancer Res* 2006;**66**:11851−8.
8. Johnson PJ, Qin SK, Park JW, Poon RTP, Raoul JL, Philip PA, et al. Brivanib *versus* sorafenib as first-line therapy in patients with unresectable, advanced hepatocellular carcinoma: results from the randomized phase III BRISK-FL study. *J Clin Oncol* 2013;**31**:3517−24.
9. Zhu AX, Park JO, Ryoo BY, Yen CJ, Poon R, Pastorelli D, et al. Ramucirumab *versus* placebo as second-line treatment in patients with advanced hepatocellular carcinoma following first-line therapy with sorafenib (REACH): a randomized, double-blind, multicenter, phase 3 trial. *Lancet Oncol* 2015;**16**:859−70.
10. Li SN, Dai WQ, Mo WH, Li JJ, Feng J, Wu LW, et al. By inhibiting PFKFB3, aspirin overcomes sorafenib resistance in hepatocellular carcinoma. *Int J Canc* 2017;**141**:2571−84.
11. Cheng AL, Kang YK, Lin DY, Park JW, Kudo M, Qin S, et al. Sunitinib *versus* sorafenib in advanced hepatocellular cancer: results of a randomized phase III trial. *J Clin Oncol* 2013;**31**:4067−75.
12. Shi J, Gao W, Shao F. Pyroptosis: gasdermin-mediated programmed necrotic cell death. *Trends Biochem Sci* 2017;**42**:245−54.
13. Ding J, Wang K, Liu W, She Y, Sun Q, Shi J, et al. Pore-forming activity and structural autoinhibition of the gasdermin family. *Nature* 2016;**535**:111−6.
14. Chen X, He WT, Hu L, Li J, Fang Y, Wang X, et al. Pyroptosis is driven by non-selective gasdermin-D pore and its morphology is different from MLKL channel-mediated necroptosis. *Cell Res* 2016;**26**:1007−20.
15. Wang Y, Gao W, Shi X, Ding J, Liu W, He H, et al. Chemotherapy drugs induce pyroptosis through caspase-3 cleavage of a gasdermin. *Nature* 2017;**547**:99−103.
16. Rogers C, Fernandes-Alnemri T, Mayes L, Alnemri D, Cingolani G, Alnemri ES. Cleavage of DFNA5 by caspase-3 during apoptosis mediates progression to secondary necrotic/pyroptotic cell death. *Nat Commun* 2017;**8**:14128.
17. Ma Z, Zhang M, Song Z. Characterization of tanshinones with quinone reductase induction activity from Radix *Salvia miltiorrhiza* by liquid chromatography/tandem mass spectrometry. *Rapid Commun Mass Spectrom* 2009;**23**:2857−66.
18. Zhou L, Jiang L, Xu M, Liu Q, Gao N, Li P, et al. Miltirone exhibits antileukemic activity by ROS-mediated endoplasmic reticulum stress and mitochondrial dysfunction pathways. *Sci Rep* 2016;**6**:20585.
19. Wang L, Hu T, Shen J, Zhang L, Li LF, Chan RL, et al. Miltirone induced mitochondrial dysfunction and ROS-dependent apoptosis in colon cancer cells. *Life Sci* 2016;**151**:224−34.
20. Wu CF, Efferth T. Miltirone induces G2/M cell cycle arrest and apoptosis in CCRF-CEM acute lymphoblastic leukemia cells. *J Nat Prod* 2015;**78**:1339−47.
21. Zhu Z. Miltirone-induced apoptosis in cisplatin-resistant lung cancer cells through upregulation of p53 signaling pathways. *Oncol Lett* 2018;**15**:8841−6.
22. Zhou X, Wang Y, Lee WY, Or PM, Wan DC, Kwan YW, et al. Miltirone is a dual inhibitor of P glycoprotein and cell growth in doxorubicin-resistant HepG2 cells. *J Nat Prod* 2015;**78**:2266−75.
23. Zhang XW, Yang L, An L, Li P, Chen J. Discovery of cancer cell proliferation inhibitors from *Salviae miltiorrhizae radix et rhizome* by a trace peak enrichment approach. *J Separ Sci* 2019;**42**:534−46.

24. Guo L, Duan L, Dong X, Dou LL, Zhou P, Liu EH, et al. A simple and sensitive LC−MS/MS method for determination of miltirone in rat plasma and its application to pharmacokinetic studies. *J Chromatogr B Analyt Technol Biomed Life Sci* 2014;**973C**:33−8.
25. Miao EA, Rajan JV, Aderem A. Caspase-1-induced pyroptotic cell death. *Immunol Rev* 2011;**243**:206−14.
26. Xie Y, Zhu S, Zhong M, Yang M, Sun X, Liu J, et al. Inhibition of aurora kinase a induces necroptosis in pancreatic carcinoma. *Gastroenterology* 2017;**153**:1429−43.
27. Shi J, Zhao Y, Wang K, Shi X, Wang Y, Huang H, et al. Cleavage of GSDMD by inflammatory caspases determines pyroptotic cell death. *Nature* 2015;**526**:660−5.
28. Van Laer L, Huizing EH, Verstreken M, van Zuijlen D, Wauters JG, Bossuyt PJ, et al. Nonsyndromic hearing impairment is associated with a mutation in *DFNA5*. *Nat Genet* 1998;**20**:194−7.
29. Lu H, Zhang S, Wu J, Chen M, Cai MC, Fu Y, et al. Molecular targeted therapies elicit concurrent apoptotic and GSDME-dependent pyroptotic tumor cell death. *Clin Canc Res* 2018;**24**:6066−77.
30. Asati V, Mahapatra DK, Bharti SK. PI3K/Akt/mTOR and Ras/Raf/MEK/ERK signaling pathways inhibitors as anticancer agents: structural and pharmacological perspectives. *Eur J Med Chem* 2016;**109**:314−41.
31. Zhang G, He J, Ye X, Zhu J, Hu X, Shen M, et al. β-Thujaplicin induces autophagic cell death, apoptosis, and cell cycle arrest through ROS-mediated Akt and p38/ERK MAPK signaling in human hepatocellular carcinoma. *Cell Death Dis* 2019;**10**:255.
32. Yang S, Liu G. Targeting the Ras/Raf/MEK/ERK pathway in hepatocellular carcinoma. *Oncol Lett* 2017;**13**:1041−7.
33. Liu C, Gong K, Mao X, Li W. Tetrandrine induces apoptosis by activating reactive oxygen species and repressing Akt activity in human hepatocellular carcinoma. *Int J Canc* 2011;**129**:1519−31.
34. Ewald F, Nörz D, Grottke A, Bach J, Herzberger C, Hofmann BT, et al. Vertical targeting of AKT and mTOR as well as dual targeting of AKT and MEK signaling is synergistic in hepatocellular carcinoma. *J Canc* 2015;**6**:1195−205.
35. Miller KD, Sauer AG, Ortiz AP, Fedewa SA, Pinheiro PS, Tortolero-Luna G, et al. Cancer statistics for hispanics/latinos. 2018 *CA Cancer J Clin* 2018;**68**:425−45.
36. Siegel RL, Miller KD, Jemal A. Cancer statistics. 2019 *CA Cancer J Clin* 2019;**69**:7−34.
37. Grandhi MS, Kim AK, Ronnekleiv-Kelly SM, Kamel IR, Ghasebeh MA, Pawlik TM. Hepatocellular carcinoma: from diagnosis to treatment. *Surg Oncol* 2016;**25**:74−85.
38. Arslanoglu A, Seyal AR, Sodagari F, Sahin A, Miller FH, Salem R, et al. Current guidelines for the diagnosis and management of hepatocellular carcinoma: a comparative review. *AJR Am J Roentgenol* 2016;**207**:W88−98.
39. Liang Y, Zheng T, Song R, Wang J, Yin D, Wang L, et al. Hypoxia-mediated sorafenib resistance can be overcome by EF24 through von Hippel-Lindau tumor suppressor-dependent HIF-1a inhibition in hepatocellular carcinoma. *Hepatology* 2013;**57**:1847−57.
40. Makin G, Dive C. Apoptosis and cancer chemotherapy. *Trends Cell Biol* 2001;**11**:S22−6.
41. Hu C, Zhang X, Wei W, Zhang N, Wu H, Ma Z, et al. Matrine attenuates oxidative stress and cardiomyocyte apoptosis in doxorubicin-induced cardiotoxicity *via* maintaining AMPKα/UCP2 pathway. *Acta Pharm Sin B* 2019;**9**:690−701.
42. Silveira TN, Zamboni DS. Pore formation triggered by *Legionella* spp. is an Nlrc4 inflammasome-dependent host cell response that precedes pyroptosis. *Infect Immun* 2010;**78**:1403−13.
43. Yu J, Li S, Qi J, Chen Z, Wu Y, Guo J, et al. Cleavage of GSDME by caspase-3 determines lobaplatin-induced pyroptosis in colon cancer cells. *Cell Death Dis* 2019;**10**:193.
44. Rogers C, Erkes DA, Nardone A, Aplin AE, Fernandes-Alnemri T, Alnemri ES. Gasdermin pores permeabilize mitochondria to augment caspase-3 activation during apoptosis and inflammasome activation. *Nat Commun* 2019;**10**:1689.
45. Dhillon AS, Hagan S, Rath O, Kolch W. MAP kinase signaling pathways in cancer. *Oncogene* 2007;**26**:3279−90.
46. Schmidt CM, McKillop IH, Cahill PA, Sitzmann JV. Increased MAPK expression and activity in primary human hepatocellular carcinoma. *Biochem Biophys Res Commun* 1997;**236**:54−8.
47. Ito Y, Sasaki Y, Horimoto M, Wada S, Tanaka Y, Kasahara A, et al. Activation of mitogen-activated protein kinases/extracellular signal-regulated kinases in human hepatocellular carcinoma. *Hepatology* 1998;**27**:951−8.
48. McDonald OB, Chen WJ, Ellis B, Hoffman C, Overton L, Rink M, et al. A scintillation proximity assay for the Raf/MEK/ERK kinase cascade: high-throughput screening and identification of selective enzyme inhibitors. *Anal Biochem* 1999;**268**:318−29.
49. Wang X, Martindale JL, Holbrook NJ. Requirement for ERK activation in cisplatin-induced apoptosis. *J Biol Chem* 2000;**275**:39435−43.
50. Sun Y, Liu WZ, Liu T, Feng X, Yang N, Zhou HF. Signaling pathway of MAPK/ERK in cell proliferation, differentiation, migration, senescence and apoptosis. *J Recept Signal Transduct Res* 2015;**35**:600−4.
51. Du X, Shi Z, Peng Z, Zhao C, Zhang Y, Wang Z, et al. Acetoacetate induces hepatocytes apoptosis by the ROS-mediated MAPKs pathway in ketotic cows. *J Cell Physiol* 2017;**232**:3296−308.
52. Zhou B, Zhang JY, Liu XS, Chen HZ, Ai YL, Cheng K, et al. Tom20 senses iron-activated ROS signaling to promote melanoma cell pyroptosis. *Cell Res* 2018;**28**:1171−85.